Title

Catalase-Containing Silica Particles as Ultrasound-Based Hydrogen Peroxide Sensors to Determine Infected From Noninfected Fluid Collections in Humans.

Journal

American Journal of Roentgenology, 213(1)

ISSN

0361-803X

Authors

Malone, Christopher D
Fetzer, David T
Lux, Jacques
et al.

Publication Date

2019-07-01

DOI

10.2214/ajr.18.20779

Peer reviewed

AJR FOCUS ON:

Catalase-Containing Silica Particles as Ultrasound-Based Hydrogen Peroxide Sensors to Determine Infected From Noninfected Fluid Collections in Humans

Christopher D. Malone[1,2]
David T. Fetzer[3]
Jacques Lux[3]
Robert F. Mattrey[3]

Keywords: abscess drainage, contrast-enhanced ultrasound, gastrointestinal imaging, molecular imaging, nanoparticles

doi.org/10.2214/AJR.18.20779

Received October 12, 2018; accepted after revision December 26, 2018.

D. T. Fetzer has research and consultation agreements with Philips Ultrasound and has been on the speakers' bureau for Philips Healthcare and Siemens Healthcare.

The content is solely the responsibility of the authors and does not necessarily represent the official views of the National Institutes of Health.

Based on a presentation at the Radiological Society of North America 2017 annual meeting, Chicago, IL.

Supported in part by the Cancer Prevention and Research Institute of Texas grant RR150010; by the Radiological Society of North America Research and Education Foundation, award RR1361; and by the National Center for Advancing Translational Sciences of the National Institutes of Health under the Center for Translational Medicine's award UL1TR001105.

[1]Department of Radiology, University of California, San Diego, San Diego, CA.

[2]Present address: Mallinckrodt Institute of Radiology at Washington University School of Medicine, St. Louis, MO.

[3]Department of Radiology, University of Texas Southwestern Medical Center, 5323 Harry Hines Blvd, Dallas, TX 75390-8514. Address correspondence to R. F. Mattrey (Robert.Mattrey@UTSouthwestern.edu).

WEB
This is a web exclusive article.

Supplemental Data
Available online at www.ajronline.org.

AJR 2019; 213:W9–W16

0361–803X/19/2131–W9

OBJECTIVE. Hydrogen peroxide (H_2O_2) plays a key role in neutrophil oxidative defense against infection. Catalase-containing silica nanoshells are nanoparticles that generate O_2 microbubbles imaged with ultrasound in the presence of elevated H_2O_2. We aimed to determine whether ultrasound-detectable O_2 microbubbles produced by catalase-containing silica nanoshells can determine whether fluid collections drained from patients are infected.

SUBJECTS AND METHODS. During this HIPAA-compliant, institutional review board–approved study, 52 human fluid samples were collected from clinically required image-guided percutaneous drainage procedures. Catalase-containing silica nanoshells were added to the fluid samples during imaging in real time using a Sequoia-512 15L8-S linear transducer (Siemens Healthcare). Production of detectable microbubbles was graded subjectively as negative (noninfected) or positive (infected) with low, moderate, or high confidence by a single observer blinded to all clinical data. The truth standard was microbiology laboratory culture results. Performance characteristics including ROC curves were calculated.

RESULTS. Microbubble detection to distinguish infected from noninfected fluids was 84% sensitive and 72% specific and offered negative and positive predictive values of 89% and 64%, respectively. The AUC was 0.79. Six of nine false-positive samples were peritoneal fluid collections that were all collected from patients with decompensated cirrhosis.

CONCLUSION. The presence of elevated H_2O_2 indicated by microbubble formation in the presence of catalase-containing silica nanoshells is sensitive in distinguishing infected from noninfected fluids and offers a relatively high negative predictive value. False-positive cases may result from noninfectious oxidative stress. Catalase-containing silica nanoshells may constitute a novel point-of-care test performed at time of percutaneous drainage, potentially obviating placement of drains into otherwise sterile collections and minimizing risk of secondary infection or other complication.

Hydrogen peroxide (H_2O_2) is a valuable biomarker of oxidative stress that has been associated with many disease states including cancer, diabetes, acute respiratory distress, and infection [1–10]. For example, H_2O_2 production as a component of leukocyte oxidative burst is a key defense mechanism against infection, with stimulated neutrophils producing up to 65 μM of extracellular H_2O_2 in solution [11]. Because infected fluid collections are rich with neutrophils and other leukocytes, we hypothesized that elevated levels of H_2O_2 in body fluids would indicate that the fluid is infected. Therefore, detection of this reactive oxygen species at bedside could serve as a valuable point-of-care (POC) tool to help manage patients with abnormal fluid collections [1, 5–7].

Current methods for detecting H_2O_2 involve fluorometric assays, such as Amplex Red (Thermo Fisher Scientific) or ferrous oxidation of xylenol orange [12]. These assays are very sensitive but unfortunately are susceptible to contamination by other body fluids, particularly blood, and are not routinely available in clinical laboratories, much less as a POC tool. Electrochemical and optical-based probes have also been developed [13–16]. However, both techniques require additional equipment and have major limitations. Electrochemical systems are affected by electrolytes and debris in the drained fluid that are difficult to control for, and optical methods have limited depth of penetration, particularly in turbid fluid and in fluid that contains blood. A reliable, low-cost sensor such as ultrasound (US) that could detect

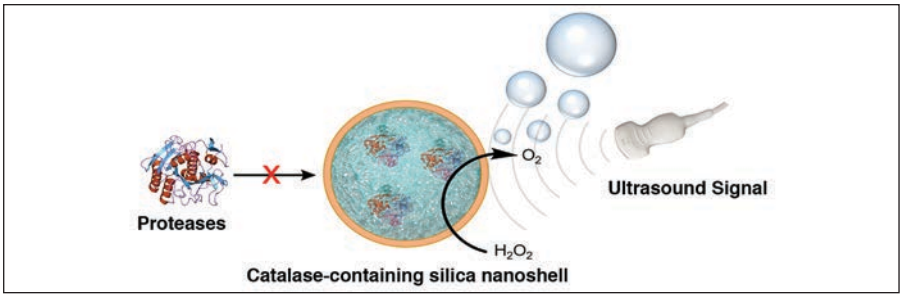

Fig. 1—Illustration depicts microbubble generation and detection when nanoparticles containing catalase are exposed to H_2O_2 during ultrasound imaging. Silica shell protects catalase from endogenous proteases while remaining porous to small molecules such as H_2O_2. After being converted to O_2 by catalase, O_2 microbubbles are generated and detected by ultrasound.

H_2O_2 at the bedside as a POC tool would be of benefit, particularly because it is commonly used to guide needle placement.

Previous reports describe nanoporous particles containing the enzyme catalase, which is capable of catalyzing H_2O_2 into oxygen (O_2) and water both in vitro and in vivo, while protecting the enzyme from degradation [17, 18]. On exposure to US, the released O_2 forms microbubbles that are detectable with standard US equipment (Fig. 1). Specifically, the use of these particles allowed the detection of H_2O_2 released by activated neutrophils in vitro and produced microbubbles detectable in vivo when injected into infectious collections within rats [17].

Minimally invasive, image-guided diagnostic and therapeutic procedures are now a routine component of modern medicine, and ultrasound is commonly used to guide percutaneous drainage procedures of fluid collections suspected to be infected [19, 20]. In this study we aimed to assess whether ultrasound can detect elevated levels of H_2O_2 in fluids aspirated from patients as a biomarker for infected fluid. Catalase-containing silica nanoshells were added to the aspirated fluid ex vivo to attempt to generate ultrasound-detectable O_2 microbubbles in the presence of H_2O_2. We hypothesized this technique could help rule out infection and eliminate the need to obligatorily place a drainage catheter into an otherwise sterile (noninfected) collection, thus providing a practical POC test that could be easily incorporated into routine clinical practice.

Subjects and Methods

Chemicals Used

Glycol chitosan (GC), deoxycholic acid (DA), 1-Ethyl-3-(3-dimethylaminopropyl)carbodiimide (EDC), *N*-Hydroxysuccinimide (NHS), catalase, tetraethyl orthosilicate (TEOS), and ammonium hydroxide (NH_4OH) were all purchased from an outside supplier and were used without further purification. Deoxycholic acid–conjugated glycol chitosan (DA-GC) and catalase-containing silica nanoshells were prepared and characterized in our laboratory as described later in this section.

Synthesis and Characterization of Deoxycholic Acid–Conjugated Glycol Chitosan

GC was modified with hydrophobic deoxycholic acid moieties to serve two purposes. First, this amphiphilic polymer was used to physically crosslink the nanogel through hydrophobic interactions. Second, the positive charge on the polymeric backbone allowed coating of the nanogel particles with silica. GC (500 mg, 2.4-mmol monomer) was dispersed in ultrapure water (50 mL) and stirred at 40°C until it dissolved completely. The resulting clear solution was then cooled to room temperature. DA (163 mg, 0.42 mmol), EDC (350 mg, 3.9 mmol), and NHS (450 mg, 3.9 mmol) were added to the solution, and the resulting mixture was stirred at room temperature for 20 hours. Ethanol (25 mL) was then added to reach 33% by volume. The final mixture was dialyzed against water for 24 hours using a cellulose ester dialysis membrane (Spectra/Por Float-A-Lyzer G2, Spectrum Laboratories; molecular weight cut-off = 3.5–5 kDa). Water was replaced four times during dialysis. The resulting solution was freeze-dried to yield 700 mg of DA-GC as a white powder. The degree of substitution of DA-GC, defined by the number of deoxycholic acid moieties conjugated to the polymer backbone per 100 monomers was determined by ^{1}H nuclear MR spectroscopy (Unity Inova 500 MHz spectrometer, Varian). Peaks corresponding to the protons of the three methyl groups of the deoxycholic acid (0.72, 0.94, and 1.01 ppm) were integrated and compared with the peaks corresponding to the protons of the monomer (3.4–4.0 ppm) to give a mean substitution ± SD of 18% ± 2.6% (Fig. S1, a supplemental figure, can be viewed in the *AJR* electronic supplement to this article, available at www.ajronline.org.).

Formulation and Characterization of Catalase-Containing Silica Nanoshells

DA-GC (12 mg) was dispersed in 6 mL of 1× phosphate-buffered saline (PBS) and heated to 70°C until it completely dissolved. The DA-GC solution was then cooled to room temperature, and 60 mg catalase (270 kU) was added. Nanogels were produced through direct high-pressure homogenization in a low-volume microfluidizer (LV1, Microfluidics) equipped with a cooling coil using three to nine cycles at 13,000 psi (89,632 kPa). Both the coil and tray were cooled with ice to avoid thermal denaturation of catalase. The mean hydrodynamic diameter of the formed nanogels was measured with dynamic light scattering (DLS) using the Zetasizer ZS nano-sizing system (Malvern Nano ZS, Malvern Instruments) and with transmission electron microscopy (TEM) (TecnaiG2 Spirit BioTWIN microscope, FEI) using negative staining with 2% uranyl acetate in water.

An aqueous solution of 1 M NH_4OH (2.6 mL) and TEOS (370 µL) were added to the nanogel suspension (6 mL), and the resulting mixture was stirred for 16 hours at room temperature. The suspension was then centrifuged at 500 × *g* to remove any large silica aggregates, and the supernatant containing the catalase-containing silica nanoshells was collected.

The mean hydrodynamic diameter and polydispersity index of the resulting catalase-containing silica nanoshells were measured by DLS while their concentration and size distribution were measured with the qNano Gold system (Izon Science), a tunable resistive pulse sensing (TRPS) instrument, using the NP300 nanopore and corresponding calibration beads. Catalase-containing silica nanoshells were further characterized by TEM using a 20-µL dilute sample on a carbon-formvar grid stained with 2% uranyl acetate negative staining solution. Finally, catalase activity was measured using the Amplex Red Catalase Assay Kit (Thermo Fisher Scientific).

In Vitro Ultrasound-Based Detection of H_2O_2 With Catalase-Containing Silica Nanoshells

The ability of catalase-containing silica nanoshells to generate microbubbles when exposed to H_2O_2 was assessed in vitro by suspending 10^{10} nanoparticles in 3 mL 1× PBS in a 3-mL plastic transfer pipette bulb containing 0.04 M sodium cholate to stabilize formed microbubbles. The transfer pipette was placed inside a tissue-mimicking sample holder composed of 1% agarose and 0.5% cornstarch in a 37°C bath and allowed to equilibrate.

Small aliquots of H_2O_2 were added to reach final concentrations of 10, 100, and 1000 μM using a transfer pipette. All solutions were introduced with the pipette tip positioned at the most nondependent aspect of the sample to prevent air from being introduced into the sample, which could be mistaken for de novo microbubbles. Samples were imaged using a clinical ultrasound scanner (Siemens Acuson Sequoia 512, Siemens Healthcare) equipped with a 15L8 transducer and contrast pulsing sequence imaging mode using a 7-MHz central transmit frequency and a mechanical index (MI) of 0.25 at 16 frames/s. The contrast pulsing sequence and B-mode images reconstructed from the same backscattered signal were displayed side by side and in cine loops recorded from before and for 1 min after the addition of H_2O_2. ImageJ software (National Institutes of Health) was used to quantify the ultrasound signal of generated O_2 microbubbles, which were detected within seconds of adding the H_2O_2. Ellipsoidal ROIs were drawn on the gray-scale US image and the log-compressed mean video intensity was measured from a mean of 40 frames acquired before and after the addition of H_2O_2. The difference in video intensity before and after adding H_2O_2 was recorded. Each H_2O_2 concentration experiment was done in triplicate.

Patient Population

We obtained approval from the institutional review board of the University of Texas Southwestern Medical Center, and the requirement of informed consent was waived. All corresponding fluids and clinical data were collected in a manner compliant with HIPAA from a single institution between February 2016 and January 2017. Any patient who had a fluid collection diagnosed on ultrasound or CT and was scheduled to undergo aspiration or drainage of the collection or who was scheduled for a therapeutic paracentesis or thoracentesis as part of that patient's clinical care was included. Paracentesis and thoracentesis fluids were included to balance the number of noninfected and infected samples to adequately power the study. Collected fluid samples were assigned a unique research identification number and transferred on ice to the laboratory, where they were stored at –80°C in a tightly capped container to arrest H_2O_2 catalysis by free catalytic enzymes or WBC peroxidases until later processing could be completed. The time from aspiration to freezing was 1 hour or less. Corresponding clinical data recorded included major medical and surgical comorbidities, clinical presentation, body location of the drained fluid, clinical laboratory findings including Gram stain, cell count and differential, and culture results. No clinical data were revealed until all H_2O_2 ultrasound detection experiments were completed and recorded. Samples were excluded from analysis if they lacked proper identification or clinical data to determine infectious status.

Evaluation of Fluid Collections

A catalase-containing silica nanoshell suspension containing 2.95×10^8 nanoshells/mL was prepared. Fluid samples were thawed, and those that were viscous or turbid were centrifuged and the supernatant tested. All H_2O_2 detection ultrasound imaging experiments were performed at 37°C with each sample placed in a 3-mL transfer pipette as was done for nanoshell characterization. Because samples can contain very low to high concentrations of H_2O_2, we performed two experiments with each sample in triplicate to maximize detection. In the first experiment, 20 μL of the catalase-containing silica nanoshell suspension were added to 0.7 mL of the sample. In the second, 20 μL of the sample were added to 0.7 mL of the suspension.

Ultrasound imaging was performed as was done for nanoshell characterization, and cine recordings were acquired immediately before and for 2–3 minutes after combining catalase-containing silica nanoshells with the fluid sample. De novo formation of microbubbles was defined as formation of new echogenic foci within the solution confirmed to be microbubbles by observing their rise toward the sample surface and their disappearance when exposed to high-power US (MI = 1.9). All fluid samples were processed and judged subjectively as either positive or negative for de novo microbubble formation by a single operator who was blinded to all clinical data. For samples deemed to be positive, a low, moderate, or high confidence level was also recorded.

Reference Standard

The classification of fluid samples as infected or noninfected was determined by a single radiologist who was not aware of the ultrasound results. All but four fluid samples were cultured for pathogens. Fluid samples were considered infected when culture was positive for microorganisms. Of the four collections not cultured, two were recorded as infected. One patient had a suspected liver abscess on imaging and a positive blood culture. The other had a symptomatic postoperative splenic bed fluid collection, and the patient improved after drainage and antibiotic treatment. Of the two samples recorded as noninfected, one was drained from a patient with a symptomatic renal cyst requiring aspiration, and the other was ascitic fluid from a patient with symptomatic large-volume ascites. A 2 × 2 table was constructed for infected versus noninfected fluids and positive versus negative microbubble formation. Sensitivity, specificity, and positive and negative

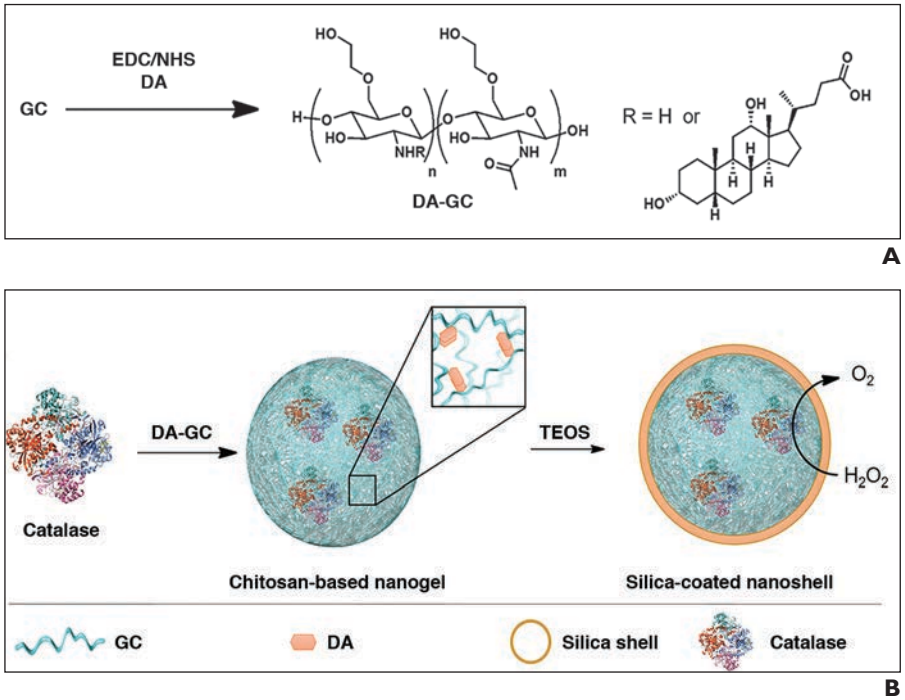

Fig. 2—Illustrations depict process of creating catalase-containing silica nanoshell.
A, Chemical reaction used to modify glycol chitosan (GC) with deoxycholic acid (DA) through 1-Ethyl-3-(3-dimethylaminopropyl)carbodiimide (EDC) and *N*-Hydroxysuccinimide (NHS) coupling reaction.
B, Schematic representation of two-step process to first formulate catalase-loaded nanogels and then silica-coated nanoshells. TEOS = tetraethyl orthosilicate.

predictive values were then calculated, and an ROC curve was constructed using the three confidence levels using Excel (version 16.15, Microsoft).

Results

Catalase-containing silica nanoshells were manufactured by producing porous DA-GC nanogels that were thereafter loaded with catalase and finally coated with silica (Fig. 2). The nanoshells had a hydrodynamic diameter of 177 nm and a polydispersity index of 0.293 as measured by DLS (Fig. 3A). One milliliter of catalase-containing silica nanoshell suspension contained 2.95×10^{10} nanoparticles as measured by TRPS (Fig. 3B). The particle size was further confirmed by TEM (Fig. 3C). Catalase activity of catalase-containing silica nanoshells was 43,650 U/mL (97% of the activity of the starting catalase before encapsulation), confirming the nondestructive catalase-containing silica nanoshell formulation process. Consequently, the 2.95×10^8 nanoshells/mL suspension used to test the samples for the presence of H_2O_2, was capable of catalyzing 436.5 μM of H_2O_2 per minute. Using graded concentrations of H_2O_2, microbubble formation was detectable by ultrasound when catalase-containing silica nanoshells were bathed in 10 μM of H_2O_2, and the number of microbubbles and corresponding video intensity increased with increasing H_2O_2 concentration (Fig. 4).

Samples from 52 patients were collected from drainage or aspiration procedures performed as part of their clinical care, 19 of which were classified as infected and 33 as not infected (Table S2, which can be viewed in the *AJR* electronic supplement to this article, available at www.ajronline.org.). When samples were positive for microbubble formation, microbubbles formed within seconds of the addition of the catalase-containing silica nanoshells. Figure 5 shows a representative case of a 44-year-old woman who presented with abdominal pain after hysterectomy and hemicolectomy and had a rim-enhancing collection within the pelvis on CT. Her fluid sample, which was positive for *Escherichia coli*, produced microbubbles on ultrasound. Results of microbubble generation from infected versus noninfected fluid samples are summarized in Table 1. Of the 19 infected samples, 16 produced detectable microbubbles with confidence levels of low (n = 3), moderate (n = 8), or high (n = 5), resulting in a sensitivity of 84% when all confidence levels are combined. Of the 33 noninfected samples, 24 did not generate microbubbles, resulting in a specificity of 73%. The negative and positive predictive values were 89% and 64%, respectively. The area under the ROC curve was 0.79 (Fig. 6).

Three false-negative results were encountered, one from a sample that was not cultured but that was labeled as infected on clinical grounds (presumed liver abscess on imaging in a patient with positive blood cultures). The second was from an abdominal fluid collection that grew *Clostridium perfringens* and other mixed gastrointestinal flora. The third was from a renal cyst that grew *E. coli*.

Of the nine noninfected samples that generated microbubbles, six were ascites samples aspirated from patients with decompensated cirrhosis. Of the remaining three samples that had a negative culture, two had elevated WBC count: One was aspirated from a peripancreatic fluid collection resulting from acute pancreatitis and complicated by pseudocyst formation, and the other was a right upper quadrant collection after partial hepatectomy complicated by bile leak. The third sample was chylous ascites following retroperitoneal lymph node dissection.

Discussion

Catalase-containing nanoshell particles help maintain catalase activity by retaining

TABLE 1: Summary of Microbubble Generation From Infected and Noninfected Fluids

Microbubble Generation	Infected	Noninfected	Total
Yes	16	9	25
No	3	24	27
Total	19	33	52

Note—Sensitivity = 84%, specificity = 73%, positive predictive value = 64%, negative predictive value = 89%.

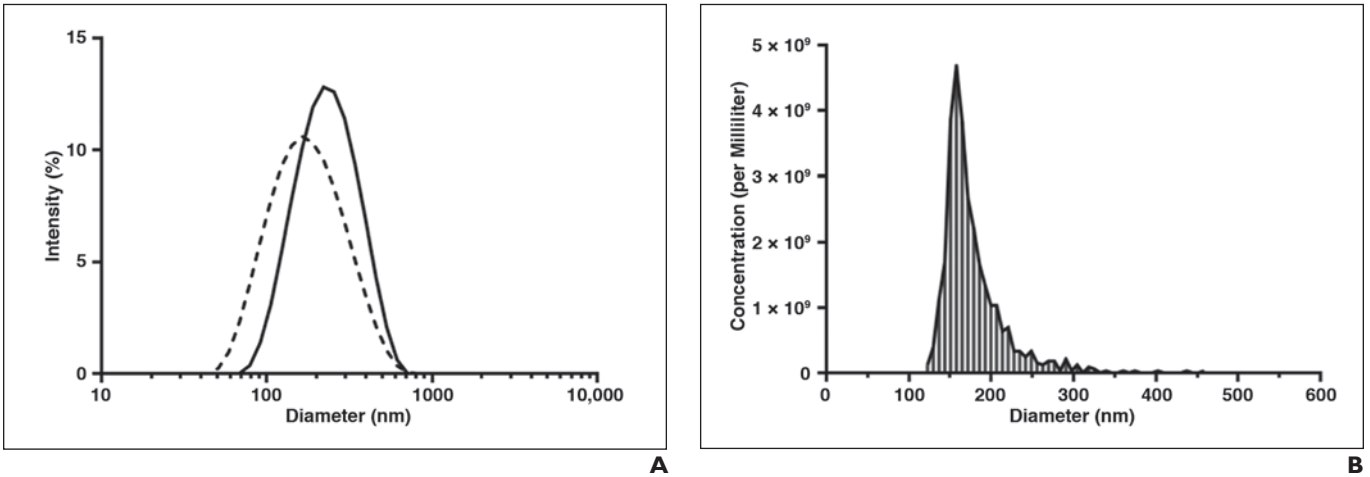

Fig. 3—Characteristics of nanogels and nanoshells used.
A, Size distribution of catalase-loaded nanogels (*dashed line*) and nanoshells (*solid line*) as measured by dynamic light scattering.
B, Size distribution and count of nanoshells as measured by tunable resistive pulse sensing.

(Fig. 3 continues on next page)

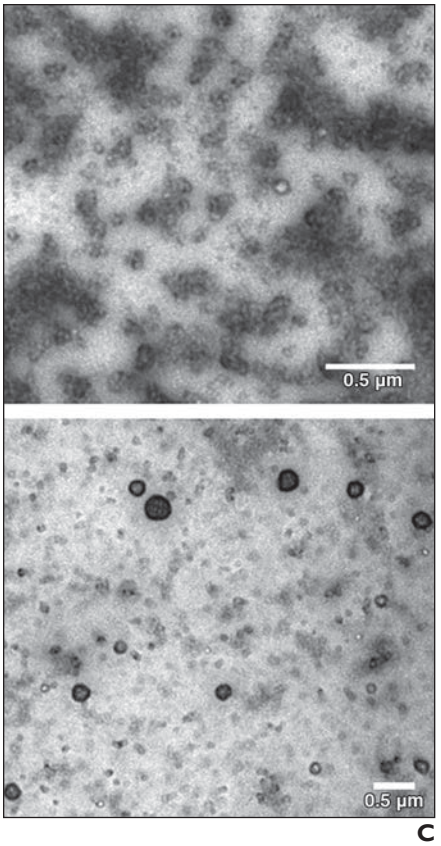

C

Fig. 3 (continued)—Characteristics of nanogels and nanoshells used.
C, Transmission electron microscopic pictures of nanogels (*top*) and nanoshells (*bottom*).

the enzyme within a hard nanoporous shell, which allows free access to small water soluble molecules, such as H_2O_2, while protecting it from macromolecules, such as endogenous proteases and antibodies. When added to solutions of H_2O_2, the catalase breaks down H_2O_2 into O_2 and water. O_2 microbubble nucleation and detection can then be achieved using clinically available ultrasound systems [17, 18]. Although catalase-containing silica nanoshells were produced using a different formulation than reported previously, they also generated O_2 microbubbles at H_2O_2 concentrations of 10 μM and above [17, 18].

In this first study geared toward translating this technique to the clinic, we hypothesized that H_2O_2 elevation could serve as a biomarker to distinguish infected from noninfected fluid collections. We were not surprised that 16 of the 19 infected collections generated microbubbles detectable by US when catalase-containing silica nanoshells were added ex vivo because inflammation, and particularly infection, recruits inflammatory cells that are known to release H_2O_2 [21]. Of the three false-negative results, one collection in the liver was not cultured and was presumed to be infected on the basis of clinical grounds, one culture was positive probably because of contamination, and the third was a renal cyst aspirate that grew *E. coli*. Although centrifuging samples to remove debris may have affected microbubble formation or detection (or both), we doubt it had an impact because imaging was done with microbubble-only imaging that subtracts signal from nonmicrobubble scatterers and because H_2O_2 is a small water soluble molecule that would reside in the supernatant that was analyzed when samples were centrifuged. High viscosity, which would require higher ultrasound pressure to nucleate microbubbles, could also have had an impact, but we do not think viscosity was a factor in this study because it would increase the false-negative rate, and only three false-negative results were seen in 19 samples. H_2O_2 levels also could have been affected by freezing and thawing of samples for analysis. Although we doubt that H_2O_2 levels could increase before analysis to yield a false-positive test, it is not clear whether the three false-negative samples were affected by endogenous catalase and WBC peroxidases that could have consumed the H_2O_2 or whether storage at –80°C affected H_2O_2 levels. We doubt that freezing had an effect because a previous study by Bortolin et al. [22] found that biologic samples were affected after freeze-thaw at –20°C but not at –80°C as was done in our study. Moreover, H_2O_2 is a small, water-soluble molecule that should not be affected by freezing. In the next study, we plan to perform the ultrasound test on aspirated fluid at the bedside, immediately after collection.

Although a negative result had at least 89% predictive value, positive results were less predictive; however, abnormally elevated levels of H_2O_2 could be used to explain other conditions in an otherwise sterile collection, such as inflammation or oxidative stress, in the proper clinical setting. Six of the nine false-positive results were from ascites samples aspirated from patients with decompensated liver disease, and two were from collections resulting from conditions known to cause significant regional inflammation (acute pancreatitis, bile peritonitis). It is intriguing to speculate that in patients with decompensated liver function from cirrhosis specifically, H_2O_2 levels could be elevated as a result of oxidative stress rather than infection, which has been implicated in increasing peritoneal permeability leading to ascites [23].

This method of detecting elevated levels of H_2O_2 at the bedside can be easily incorporated into interventional procedures, particularly because ultrasound is portable and commonly used to guide needle aspiration and drainage catheter placement. The most rapid and available method to predict whether a fluid is infected is based on results of a Gram stain performed on fluid immediately after aspiration, which may take up to 30 minutes and require close coordination with the microbiology laboratory. The method presented here yielded a higher specificity and comparable sensitivity for detection of infected fluids than a method used by Ketai et al. [19] that incorporated results of a Gram stain, WBC count in the fluid, and whether fluid was visually purulent [19]. In contrast, detection of elevated levels of H_2O_2 would be available immediately, acting as a POC test in the proper clinical setting. Although a host of biosensors have been developed to detect infectious diseases, they require sample preparation, ability to handle heterogeneous and complex fluids, specific hardware development, and, equally challenging, implementation into the clinical infrastructure and workflow [24].

The decision to place a drainage catheter into a collection presumed to be infected because of the presence of H_2O_2 is supported by the relatively high negative predictive value achieved in this study. Should this re-

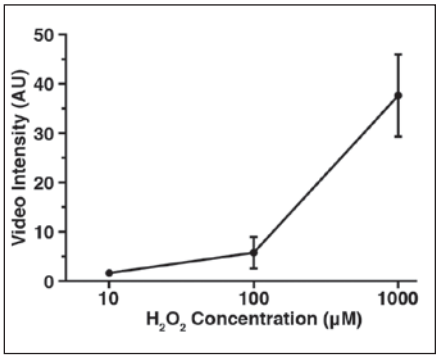

A

Fig. 4—Increasing ultrasound signal intensity from O_2 microbubbles generated from catalase-containing silica nanoshells correlated with H_2O_2 concentration.
A, Video intensity measured at various concentrations of H_2O_2.

(Fig. 4 continues on next page)

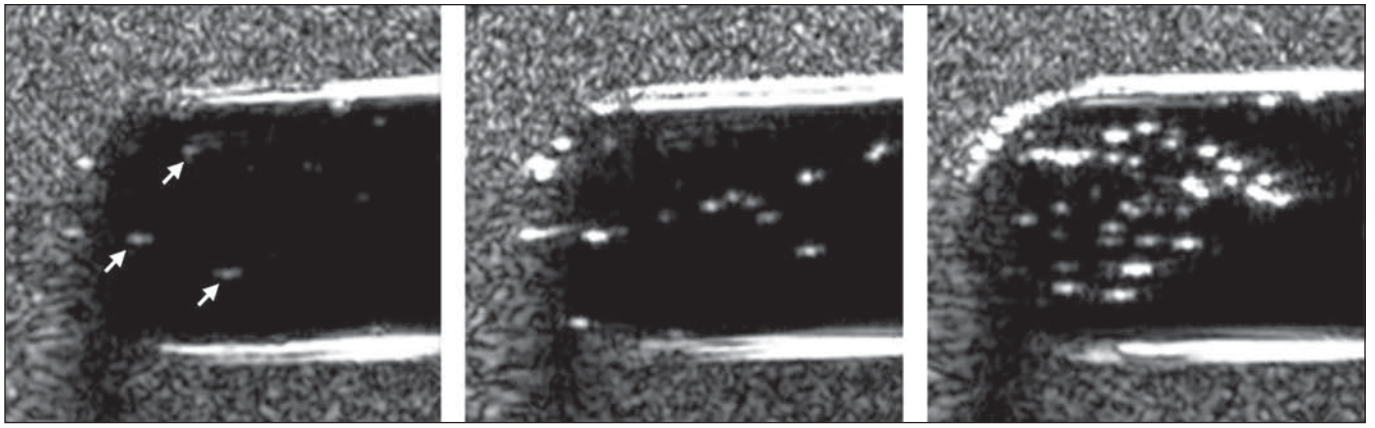

B

Fig. 4 (continued)—Increasing ultrasound signal intensity from O_2 microbubbles generated from catalase-containing silica nanoshells correlated with H_2O_2 concentration. **B,** Representative images of O_2 microbubbles (*arrows*) generated at 10 (*left*), 100 (*middle*), and 1000 (*right*) μM of H_2O_2.

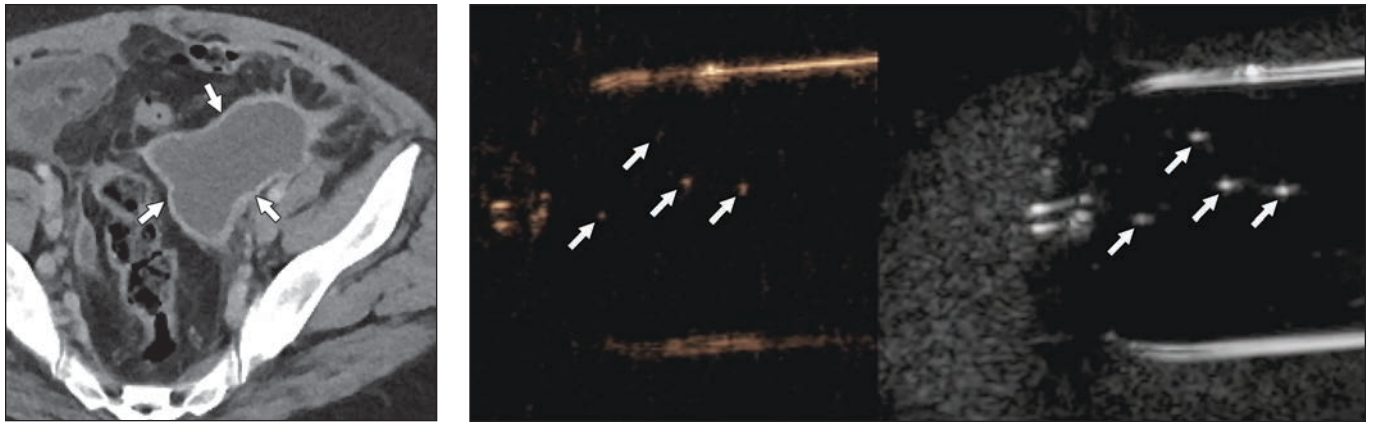

A B

Fig. 5—44-year-old woman with abdominal pain after hysterectomy and hemicolectomy.
A, CT scan obtained before drainage procedure shows rim-enhancing fluid collection in left lower quadrant (*arrows*). Culture of drained fluid grew *Escherichia coli*.
B, On contrast mode (*left*) and B-mode (*right*) ultrasound, catalase-containing silica nanoshells added to aliquot of this collection resulted in generation of O_2 microbubbles (*arrows*) from pathophysiologic levels of H_2O_2.

sult be supported by a larger study, it would obviate the placement of drains into otherwise sterile collections, thus minimizing risk of contamination, secondary infection, or other complications. This advantage is particularly pertinent for drainage of subdiaphragmatic collections, which carry the risk of traversing the pleura with a large drainage catheter [25]. Nearly half of fluid collections after abdominal surgery are not infected [26]. Although placing a drainage catheter over simple aspiration of sterile pancreatic collections yielded no clinical benefit, long-term catheter placement resulted in bacterial colonization in more than 50% of cases [27]. Further benefit of not draining sterile collections is that half of collections that develop after pancreatic surgery are asymptomatic or resolve spontaneously [28]. Therefore, there is clear clinical benefit in recognizing which fluid collections need further drainage.

Whether this POC test could be used to guide drainage decisions will require additional prospective clinical studies. We anticipate that in the initial phase of development, our approach can be incorporated as an ex vivo test to avoid regulatory hurdles and biologic safety concerns about catalase-containing silica nanoshells, speeding translation. In the long term, catalase-containing silica nanoshells may be able to be incorporated into the aspiration needle to test for the presence of H_2O_2 by ultrasound in vivo.

Our study had several limitations. First, three of the 52 samples were not cultured and assignment as infected or not infected was made on a clinical basis. Further, some samples were collected from patients during the course of their illness when antibiotic therapy or other interventions may have been initiated, potentially affecting the utility of culture results [29]. Regardless of whether antibiotic therapy was initiated, particularly in septic patients, our test only evaluates for the presence of H_2O_2 [30]. Because H_2O_2 is naturally catalyzed in extracellular fluid and plasma and eliminated in urine, the continued presence of H_2O_2 after intervention, which renders our test positive, suggests continued H_2O_2 production and therefore continued inflammation. Second, only one observer assessed the production of microbubbles on ultrasound after the addi-

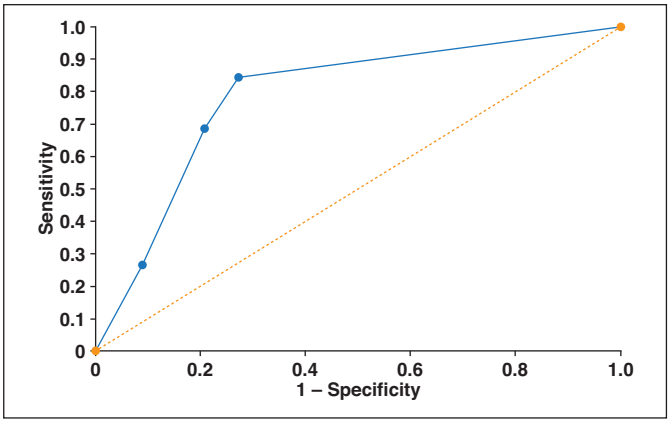

Fig. 6—ROC curve (*solid line*) from catalase-containing silica nanoshell microbubble generation in distinguishing infected from noninfected fluids. AUC = 0.79. Dotted line denotes AUC of 0.5.

tion of catalase-containing silica nanoshells in this pilot study. Future studies will need to evaluate interobserver variability. Third, though microbubble production in the presence of H_2O_2 has been well documented in the literature, and in this study quantification of H_2O_2 levels in the fluid samples was not possible [17, 18, 31]. Amplex Red assay was unreliable because of several factors including biologic complexity of aspirate, sample heterogeneity, and contamination by blood that interferes with the fluorescence readout [32]. Electrochemical methods for H_2O_2 quantification were also significantly limited by the heterogeneous complex biologic samples that had high background electrical signal, in part because of the variability in electrolyte content.

Conclusion

Elevated H_2O_2, as shown by ultrasound detection of O_2 microbubble formation in the presence of catalase-containing silica nanoshells, is sensitive for distinguishing infected from noninfected fluids and may serve as a tool in detecting high oxidative stress. Most importantly, lack of microbubble detection carried an 89% negative predictive value for ruling out infection, which may help avoid placing a draining catheter into an otherwise noninfected collection, minimizing unnecessary cost and risk. With formulation and procedure optimization, this test may become more predictive. The proposed bedside technique is advantageous over fluorescence or electrochemical methods for H_2O_2 detection because it uses conventional US images as its readout. Although this study had limitations, our results are encouraging and help justify the optimization of this POC procedure to facilitate a larger prospective study to assess potential impact on patient management decisions.

References

1. Banerjee D, Madhusoodanan UK, Nayak S, Jacob J. Urinary hydrogen peroxide: a probable marker of oxidative stress in malignancy. *Clin Chim Acta* 2003; 334:205–209
2. Banerjee D, Jacob J, Kunjamma G, Madhusoodanan UK, Ghosh S. Measurement of urinary hydrogen peroxide by FOX-1 method in conjunction with catalase in diabetes mellitus: a sensitive and specific approach. *Clin Chim Acta* 2004; 350:233–236
3. Chandramathi S, Suresh K, Anita ZB, Kuppusamy UR. Comparative assessment of urinary oxidative indices in breast and colorectal cancer patients. *J Cancer Res Clin Oncol* 2009; 135:319–323
4. Ostrow V, Wu S, Aguilar A, Bonner R Jr, Suarez E, De Luca F. Association between oxidative stress and masked hypertension in a multiethnic population of obese children and adolescents. *J Pediatr* 2011; 158:628–633
5. Halliwell B, Long LH, Yee TP, Lim S, Kelly R. Establishing biomarkers of oxidative stress: the measurement of hydrogen peroxide in human urine. *Curr Med Chem* 2004; 11:1085–1092
6. Halliwell B, Clement MV, Long LH. Hydrogen peroxide in the human body. *FEBS Lett* 2000; 486:10–13
7. Mathru M, Rooney MW, Dries DJ, Hirsch LJ, Barnes L, Tobin MJ. Urine hydrogen peroxide during adult respiratory distress syndrome in patients with and without sepsis. *Chest* 1994; 105:232–236
8. Chandramathi S, Suresh K, Anita ZB, Kuppusamy UR. Elevated levels of urinary hydrogen peroxide, advanced oxidative protein product (AOPP) and malondialdehyde in humans infected with intestinal parasites. *Parasitology* 2009; 136:359–363
9. Yuen JW, Benzie IF. Hydrogen peroxide in urine as a potential biomarker of whole body oxidative stress. *Free Radic Res* 2003; 37:1209–1213
10. Puertollano MA, Puertollano E, de Cienfuegos GÁ, de Pablo MA. Dietary antioxidants: immunity and host defense. *Curr Top Med Chem* 2011; 11:1752–1766
11. Test ST, Weiss SJ. Quantitative and temporal characterization of the extracellular H2O2 pool generated by human neutrophils. *J Biol Chem* 1984; 259:399–405
12. Rhee SG, Chang TS, Jeong W, Kang D. Methods for detection and measurement of hydrogen peroxide inside and outside of cells. *Mol Cells* 2010; 29:539–549
13. Tamasko M, Nagy L, Mikolas E, Molnar GA, Wittmann I, Nagy G. An approach to in situ detection of hydrogen peroxide: application of a commercial needle-type electrode. *Physiol Meas* 2007; 28:1533–1542
14. Aran K, Parades J, Rafi M, et al. Stimuli-responsive electrodes detect oxidative stress and liver injury. *Adv Mater* 2015; 27:1433–1436
15. Karton-Lifshin N, Segal E, Omer L, Portnoy M, Satchi-Fainaro R, Shabat D. A unique paradigm for a Turn-ON near-infrared cyanine-based probe: noninvasive intravital optical imaging of hydrogen peroxide. *J Am Chem Soc* 2011; 133:10960–10965
16. Wang H, Park SM. Polypyrrole-based optical probe for a hydrogen peroxide assay. *Anal Chem* 2007; 79:240–245
17. Olson ES, Orozco J, Wu Z, et al. Toward in vivo detection of hydrogen peroxide with ultrasound molecular imaging. *Biomaterials* 2013; 34:8918–8924
18. Olson ES, Ortac I, Malone C, Esener S, Mattrey R. Ultrasound detection of regional oxidative stress in deep tissues using novel enzyme loaded nanoparticles. *Adv Healthc Mater* 2017; 6:1601163
19. Ketai L, Washington T, Allen T, Rael J. Is the stat Gram stain helpful during percutaneous image-guided fluid drainage? *Acad Radiol* 2000; 7:228–231
20. Chemaly RF, Hall GS, Keys TF, Procop GW. Microbiology of liver abscesses and the predictive value of abscess gram stain and associated blood cultures. *Diagn Microbiol Infect Dis* 2003; 46:245–248
21. Nauseef WM. Myeloperoxidase in human neutrophil host defence. *Cell Microbiol* 2014; 16:1146–1155
22. Bortolin RC, Gasparotto J, Vargas AR, et al. Effects of freeze-thaw and storage on enzymatic activities, protein oxidative damage, and immunocontent of the blood, liver, and brain of rats. *Biopreserv Biobank* 2017; 15:182–190
23. Udwan K, Brideau G, Fila M, Edwards A, Vogt B, Doucet A. Oxidative stress and nuclear factor κB (NF-κB) increase peritoneal filtration and contribute to ascites formation in nephrotic syndrome. *J Biol Chem* 2016; 291:11105–11113
24. Sin ML, Mach KE, Wong PK, Liao JC. Advances and challenges in biosensor-based diagnosis of infectious

diseases. *Expert Rev Mol Diagn* 2014; 14:225–244

25. Neff CC, Mueller PR, Ferrucci JT Jr, et al. Serious complications following transgression of the pleural space in drainage procedures. *Radiology* 1984; 152:335–341
26. Gnannt R, Fischer MA, Baechler T, et al. Distinguishing infected from noninfected abdominal fluid collections after surgery: an imaging, clinical, and laboratory-based scoring system. *Invest Radiol* 2015; 50:17–23
27. Walser EM, Nealon WH, Marroquin S, Raza S, Hernandez JA, Vasek J. Sterile fluid collections in acute pancreatitis: catheter drainage versus simple aspiration. *Cardiovasc Intervent Radiol* 2006; 29:102–107
28. Sierzega M, Kulig P, Kolodziejczyk P, Kulig J. Natural history of intra-abdominal fluid collections following pancreatic surgery. *J Gastrointest Surg* 2013; 17:1406–1413
29. Wang YC, Wong CB, Wang IC, Fu TS, Chen LH, Chen WJ. Exposure of prebiopsy antibiotics influence bacteriological diagnosis and clinical outcomes in patients with infectious spondylitis. *Medicine (Baltimore)* 2016; 95:e3343
30. Mazuski JE, Tessier JM, May AK, et al. The Surgical Infection Society revised guidelines on the management of intra-abdominal infection. *Surg Infect (Larchmt)* 2017; 18:1–76
31. Yang F, Hu S, Zhang Y, et al. A hydrogen peroxide-responsive O_2 nanogenerator for ultrasound and magnetic-resonance dual modality imaging. *Adv Mater* 2012; 24:5205–5211
32. Tarpey MM, Fridovich I. Methods of detection of vascular reactive species: nitric oxide, superoxide, hydrogen peroxide, and peroxynitrite. *Circ Res* 2001; 89:224–236

FOR YOUR INFORMATION

The data supplement accompanying this web exclusive article can be viewed by clicking "Supplemental" at the top of the article.